Middle East Journal of Applied Sciences
Volume: 12 | Issue: 02| April – June | 2022

EISSN: 2706 -7947 ISSN: 2077- 4613
DOI: 10.36632/mejas/2022.12.2.18
Journal homepage: www.curresweb.com
Pages: 171-181

Using Double Layer Hydroxides Grafted With EDTA for Removal of Some Heavy Metals from Groundwater

Ahmed M. Desouky and Mohamed E.A. Ali

Hydrogeochemistry Department, Desert Research Center, Cairo, Egypt

Received: 10 May 2022 **Accepted:** 15 June 2022 **Published:** 30 June 2022

ABSTRACT

EDTA· Mg-Al LDH that had an intercalated in the interlayer of Mg-Al LDH, could be synthesized by adding a solution of $Mg(NO_3)_2$ and $Al(NO_3)_3$ to a solution of NaOH and EDTA -2Na (disodium-EDTA). The effect of the NaOH concentration in the solution on the formation of EDTA ·Mg-Al LDH was examined to control the chemical species of the EDTA incorporated in the interlayer. The synthesized EDTA· Mg-Al LDH was found to have a capacity for rapid uptake of Fe^{2+} and Pb^{2+} from an aqueous solutions. Batch experiments were conducted to study the effects of pH, shaking time. The results reveal that the maximum adsorption capacity is 85.71 and 109.21 mg g^{-1}. which displaying a high efficiency for the removal of Fe^{2+} and Pb^{2+} from aqueous solution. The adsorption follows Langmuir model and pseudo-second-order kinetics.

Keywords: double layer hydroxides, EDTA, Water treatment, Heavy metals, Removal

1. Introduction

Because of their accumulation (in both effluents and the environment), the use of chemicals leads to serious environmental problems directly or indirectly (Zaghloul *et al.*, 2019). Water pollution can mainly be divided into three categories: inorganics, organic and microorganisms. Heavy metals as part of inorganic pollution is considered a worldwide issue due to their harmful effects on environment including human beings (Lu Xiao *et al.,* 2021). Various technologies including chemical precipitation (Jing *et al*., 2018), coagulation and flocculation, electrochemical methods, reverse osmoses, membrane separation and ion exchange (Rafiq *et al.,* 2021) [4].Layered double hydroxides (LDH), the structure of these materials as well as their high anionic exchange capacity make them suitable for many applications (Camilo *et al.,*2021) such as the sorption of many inorganic and organic anions (Pavlovic *et al.,*2005), potential contaminants of waters. They consist of layers and are represented by the general formula $[M^{II}_{1-x} M^{III}_{x} (OH)_2]^{x+} (A^{n-})_{x/n} \cdot mH_2O$, where cationic MII and MIII are divalent and trivalent metals and occupy the octahedral holes in the brucite-like layer. An^- is the interlayer exchangeable anions, which is located in the hydrate layered galleries, and x is the layer charge density $x = [M^{II}] / ([M^{III}] + [M^{III}])$ (Naoki and Shuang, 2018). The layered structure of LDHs is shown in Fig 1. Recently, some authors reported about LDH containing chelating agents such as etilendiaminetetraacetate, EDTA and nitrilotriacetate, NTA, as well as the metal cations uptake by these materials (Reza *et al.,* 2021) .Heavy metal ions in wastewaters and their toxicity gradually arouse the attention of the whole world (Jingwan *et al.,* 2021; Wen *et al.,* 2018 and Bolan *et al.,* 2017). Heavy metals in chemistry refer to those metals with a relatively high atomic number, atomic weight, and a density>5 g/cm^3 (Pourret and Bollinger, 2018). They can be classified into three categories: toxic metals, precious metals and radioactive metals (Bansod *et al.,* 2017). The toxic metals are one of the most important pollutants of both natural and treated water (Mohammad *et al.,* 2019). Because of higher solubility in the aquatic environment, heavy metals can easily be absorbed by living organisms and thus can possibly get accumulated in their body and concentrate throughout the food chain (Arshid *et al.,* 2019). Lead and iron ions are heavy metals with deleterious effects on biological health even at low concentrations (Naja and Volesky, 2009; Yang *et al.,* 2019). Children and pregnant women are more

Corresponding Author: Ahmed M. Desouky, Hydrogeochemistry Department, Desert Research Center, Cairo, Egypt. E-mail: ahmeddesouky_27@hotmail.com

vulnerable to toxic metals: ingestion of lead can cause slow growth, anemia and even mortality in children, increased kidney dysfunction and hypertension in adults. Polluted drinking water could be a silent killer (Sidi *et al.,* 2020). Layered double hydroxides (LDHs) are an attractive class of cheap and nontoxic clay materials (Zhou *et al.,* 2021). Upon modification, LDHs exhibited more diverse functional groups, a higher specific surface area, and a larger adsorption capacity for heavy. Functional groups can serve as sorption sites to bind pollutants and are essential for the adsorption abilities of LDHs (Dhal *et al.,* 2013). Functional groups can affect adsorption affinities via electrostatic attraction, chelating action, and hydrogen-bond interactions (Yuan *et al.,* 2013).The abundant hydroxyl, carboxyl and amine groups of ethylenediaminetetraacetic acid (EDTA) metals (Jing *et al.,* 2020). In this study, we synthesized and characterized EDTA intercalated MgAl-LDH. The capture performance of LDH-EDTA for Fe^{+2} and Pb^{+2} in treatment and evaluated through batch adsorption experiments. Based on experimental and characteristic results, of adsorption on LDH-EDTA was further investigated. The validity of LDH-EDTA was evaluated in real pollutant treatment.

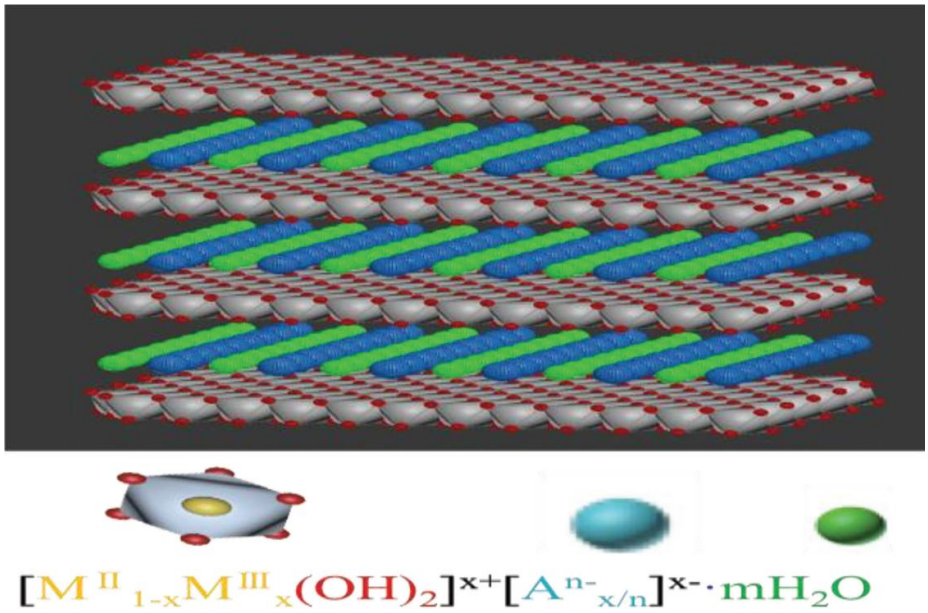

Fig. 1: The layered structure of LDHs.

2. Materials and methods

2.1. Preparation of Mg-Al LDH

The Mg–Al LDH was synthesised by following the method (Rajib *et al.,* 1998). A 188.32 g 0.502 M. of Al $(NO3)_3$.$9H_2O$ and 230.79 g 0.9 M. of Mg $(NO3)_2$. $6H_2O$ were dissolved in 700 cm^3 water. A mixture of 280 cm^3 of 12.5 M NaOH solution and 1000 cm^3 of 1 M Na_2 CO_3 solution was added in drops over a period of 4 h under stirring condition maintaining a pH of 9.5 with stirring for 24 h at 150 °C. The product was filtered, washed free of sodium ion and dried at 70 °C for 24 h in an air oven.

2.2. Preparation of Mg–Al-LDH-EDTA

EDTA-intercalated MgAl-LDH was obtained through a simple coprecipitation process. The EDTA powder (12.284 g) was dissolved in 100 mL distilled water with ultrasonic dispersion, and the $Mg(NO_3)2.6H_2O$ (33.874 g) and Al(NO3)$3.9H_2O$ (24.759 g) were added into 100 mL distilled water, respectively. The pH value of the mixed solution was kept at 10.5 by using NaOH solution (1.0 mol/L). the above mixture was mixed uniformly for 1 h. Finally, the homogeneous suspension was dried at 50°C. After aging for 24 h, distilled water was used to wash the precipitate (Hai *et al.,* 2018).

2.3. Characterization of Mg–Al-LDH-EDTA

The formation of additional functional groups on Mg–Al-LDH-EDTA was studied FTIR-spectroscope , Scanning electron micrographs (SEM) and X-ray.

Infrared spectroscopy was carried out using Gensis Unicam FT-IR spectrophotometer by incorporating the sample in a KBr disk. Scanning electron micrographs (SEM), Quanta FEG 250 microscope. High angle X-ray diffraction (XRD) patterns were recorded on X-ray diffractometer (D/Max2500VB2+/Pc, Rigaku, Japan) with Cu Kα characteristic radiation (wavelength = 0.154 nm) at a voltage of 40 kV and a current of 50 mA. The scanning rate was 5◦/min and the scanning scope of 2θ was from 5◦ to 70◦ at room temperature

2.4. Batch adsorption tests

Applicability of Mg–Al-LDH-EDTA for Pb(II) and Fe(II) removal was studied using batch experiments in a reaction mixture of 0.25 g of adsorbent and 50 ml of metal solution containing Pb(II) and Fe(II) at concentrations ranging from 100 to 500 mgL^{-1}. The effect of pH was studied at metal concentration of 100 mgL^{-1} in the pH range of 2–5. The effect of contact time was studied at metal concentrations of 200 mgL^{-1}. Agitation was undertaken using a rotary shaker type SK 300 (Lab companion). At designated contact time, the adsorbent was separated from the solution. The metal concentrations in the filtrates were analyzed by inductive coupled plasma Mass Spectrometry (ICP-MS). The adsorption capacities (mg g^{-1}) of modified chitosan were calculated as follows:

$$qe = (C_i - C_e)\, V(L)/W \qquad (1)$$

Where C_i and C_e are the initial and the equilibrium concentrations, respectively (mg L^{-1}), while W(g) and V (L) represent the weight of the adsorbent and the volume of the solution, respectively.

3. Results and Discussion

3.1. Characterization of Mg–Al-LDH-EDTA

The presence of additional functional groups on the surface of MgAl-EDTA-LDH was studied using FTIR spectroscopy (Fig. 2).

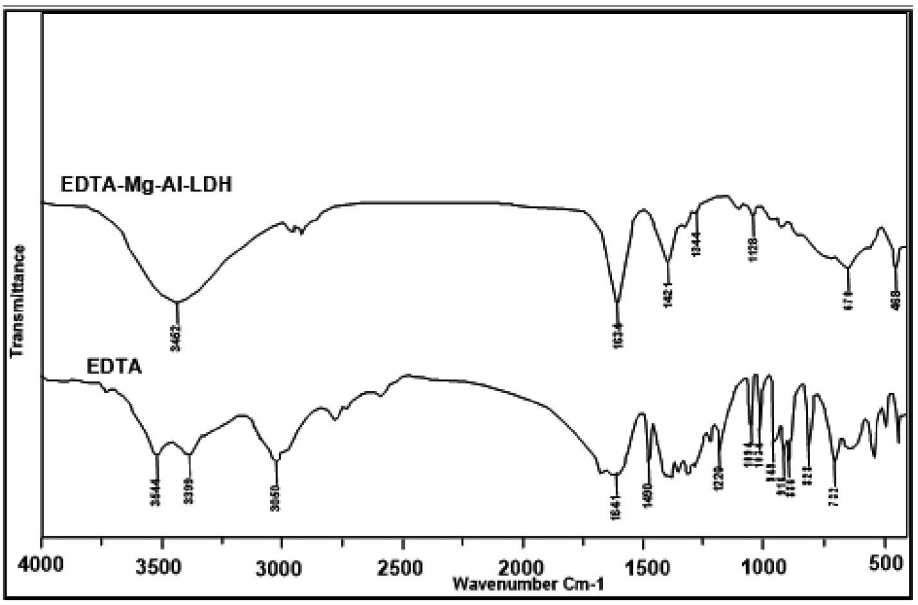

Fig. 2: IR shows of the samples EDTA and MgAl-EDTA-LDH

The broad absorption band atabout 34452 cm^{-1} is assigned to (OH) stretching modes of freeand hydrogen-bonded hydroxyl groups. The bands observed at the lower frequency, around 670 and 468 cm^{-1}, correspond to the lattice vibration modes and are attributable to (M-O) and (M-O-M), respectively. The features located at 1634 and 1421 cm^{-1} are assigned to carboxylate (COO−) asymmetric and symmetric stretching modes, respectively. Bands at 1344 and 1128 cm^{-1} are characteristic of $CH_2$and C-N groups, respectively (Yuan *et al.,* 2013). The position of these bands

corresponds to the EDTA functional groups.The XRD analyses were applied to characterize the synthesis samples and confirm that EDTA is intercalated intoMgAl-NO3-LDH. Fig. 3 shows the XRD patterns of MgAl-LDH,MgAl-EDTA-LDH. The diffraction peaks of MgAl-NO3-LDH are typical of the layered dou-ble hydroxides structure with sharp and symmetric reflections of the basal (003), (006) and (009) planes, and broad, less intense and asymmetric reflections for the nonbasal (015) and (018) planes (Hong *et al.,* 2018). The MgAl-EDTA-LDH still retains the characteristics of LDH nanoplates structure after the intercalation of EDTA in MgAl-NO_3-LDH, but there are spacing of some planes as (003), (006) and (009) plane was changed in width and intensity, because of interlayer space occupied by EDTA anions.

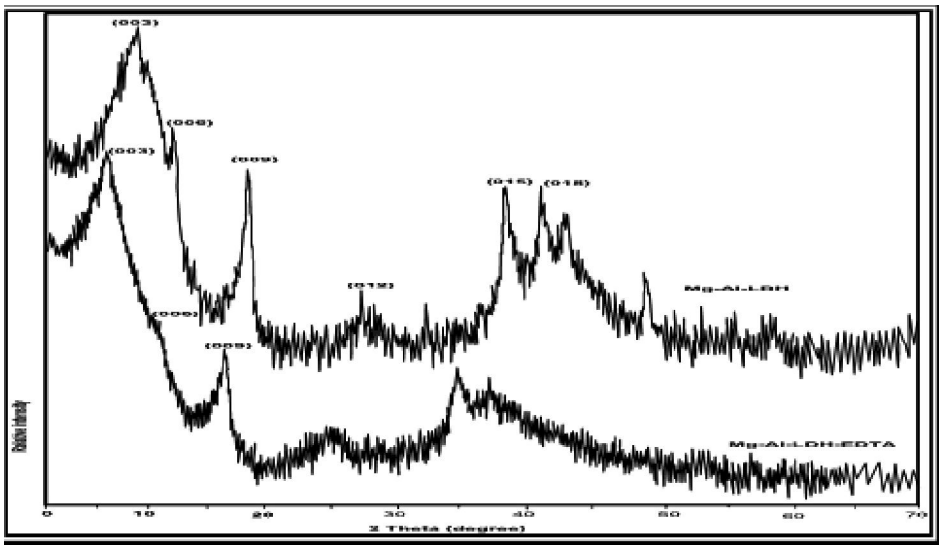

Fig. 3: Shows the XRD patterns of MgAl-LDH,MgAl-EDTA-LDH.

Fig. 4. 4 (A,B) SEM images of Mg–Al LDH, MgAl-EDTA-LDH powders that shown their microstructures in Fig. 3A, it can be clearly observed that the surface was rough and in Fig. 3B. The more crystalline carbonate phase [Fig. 3B] shows layers of sub-micrometre-sized particles. These particles have approximately aggregated into a large platy mass, and compact regular pore structure. Due to its structure and high surface area, Fig. 4B displays smooth lamellar structure of EDTA intercalated into Mg–Al LDH, indicating the typical morphology of LDHs, in summary, the MgAl-EDTA-LDH were synthesized successfully.

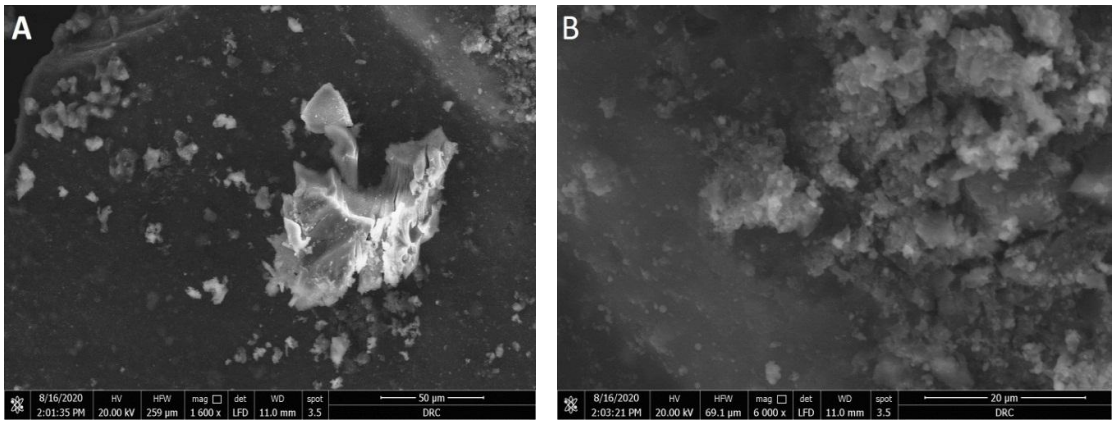

Fig. 4: (A) SEM images of Mg–Al LDH, (B) MgAl-EDTA-LDH powders

3.2. Effects of pH

The acidity of the aqueous solution exerts profound effect on the adsorption process because it can influence the solution chemistry of contaminants and the properties of the adsorbent. The effect of solution pH on Fe (II) and Pb(II) adsorption was investigated at pH 2-5. So the effect of solution pH on metal ions removal after socking of 24 hr, by adjusting the solution pH using 0.1N HCl or 0.1N NaOH. Fig 5 shows the effect of pH on the individual adsorption of Fe (II) and Pb(II) by MgAl-EDTA-LDH. The adsorption increases with increasing the pH value up to 5 where the maximum adsorption were obtained.

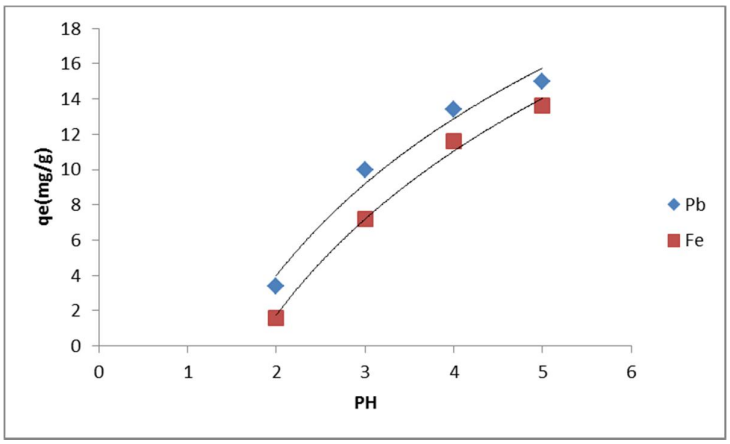

Fig. 5: pH-dependent metal uptake of metal ions.

The low adsorption of metal ions in strong acidic pH solution (at low pH) could be mainly due to the electrostatic repulsion between the positive metal ions (M^+) in the medium and the positive charges in highly acidic solution (H^+) which accumulate on the surface of the MgAl-EDTA-LDH, also At a very low pH, the structures of MgAl-EDTA-LDH were impaired that resulted in the dissolution of Mg^{2+} from MgAl-EDTA-LDH,so protonated ions, reducing the number of binding sites available for the adsorption of heavy metal ions. This leads to the inducing an electrostatic repulsion of the different heavy metal ions. Therefore, the competition existed between protons and the metal ions (M^+) for adsorption sites and adsorption capacity was decreased. Such repulsion prevents the approach of the metal ions to MgAl-EDTA-LDH surface. While at higher pH value, the adsorption capacities of Pal/MgAl–LDH for metal ions were enhanced because of exerting the synergetic effect from each building unit. Also, the adsorption of, Fe^{2+} and Pb^{2+} on MgAl-EDTA-LDH showed that calcination could improve the adsorption performance. Further increase in the pH value more than 5 would transform the dissolved metal into precipitated hydroxide form thus the adsorption capacity is decreased (Eslam *et al.,* 2019).

3.3. Effects of contact time

The effect of contact time on Fe (II) and Pb (II) adsorption by MgAl-EDTA-LDH are shown in Fig. 6. In the first few min, the adsorption capacities of MgAl-EDTA-LDH increased sharply. Then, the removal rates slowed down and finally reached equilibrium states.

Within the first few minutes, the active sites of the adsorbents were sufficient for Fe (II) and Pb (II) adsorption and the direct electrostatic attractions of them also occurred. With the increase of time, more and more active adsorption sites were occupied by the target pollutant, and the chelation of Fe (II) and Pb (II) with EDTA anions contributed to the removal process.

3.4. Regeneration studies

Regeneration of the spent adsorbent is necessary to restore its original adsorption capacity and it enables valuable metals to be recovered from wastewater streams for reuse. In this study, Pb (II) and Fe(II) were desorbed from MgAl-EDTA-LDH using 1M HNO_3. From Table 1 we can suggests that the regeneration efficiency of both adsorbents was almost complete for both metals. These results indicate the suitability of HNO_3 as the regenerant for the adsorbent. It seems that the adsorption efficiency of the MgAl-EDTA-LDH decreased with repeating cycles, several possible reasons for decreasing cation

exchange capacity of MgAl-EDTA-LDH have been discussed. First, the little amount of Pb (II) and Fe(II) ions still remained on the MgAl-EDTA-LDH surface after every regeneration cycle. Second, the active efficient groups on the MgAl-EDTA-LDH were partially destroyed by HNO_3 after every regeneration cycle. These could lead to decreasing the performance of adsorption (Facui *et al.,* 2016).

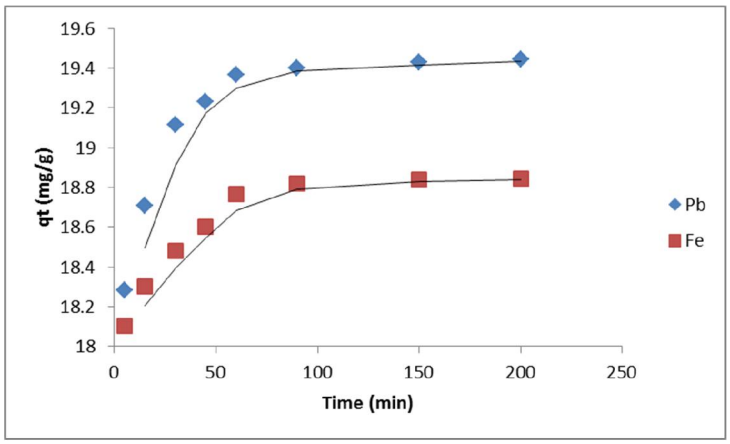

Fig. 6: Metal uptake of metal ions with time.

Type of adsorbent	No. of cycles	RE% Pb (II)	RE% Fe (II)
MgAl-EDTA-LDH	1	98.00	96.90
	2	97.80	95.86
	3	97.20	95.76
	4	97.10	95.4
	5	96.50	95.20

3.5. Adsorption kinetics

To describe the relationship between the adsorption capacity and contact time to analyze the adsorption mechanism and better understand the potential rate-limiting step, pseudo-first-order, pseudo-second-order, kinetic models are employed to fit the experimental data. All the kinetic data are shown in Fig. 7 and Table 1, the pseudo-first-order model is expressed as (Ahmed, 2018):

$$\text{Log } (q_e - q_t) = \log q_e - \frac{k1}{2.303} t$$

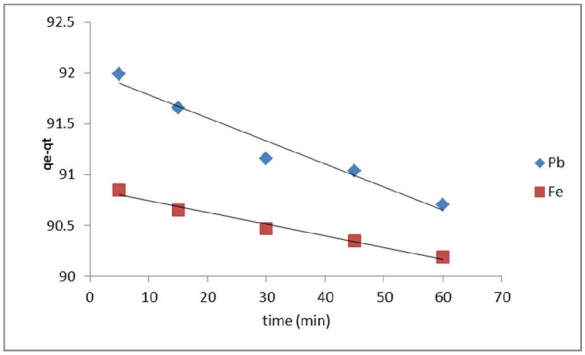

Fig. 7: Plots of log(qe-qt) ainst time for the exchange of Fe(II) and Pb(II) ions on MgAl-EDTA-LDH.

and pseudo-second-order rate equation is:

$$\frac{t}{qt} = \left(\frac{1}{k2qe2}\right) + \frac{1}{qe} t$$

Where k1 and k2 ($g \cdot mg^{-1} \cdot min^{-1}$) are rate constants for adsorption. R^2 is the correlation coefficient to express the uniformity between the model-predicted values and the experimental data. The linear regressions and kinetic parameters are listed in Fig. 8 and Table 2, respectively. It is clear that

correlation coefficients for the pseudo-second-order model (R^2>0.99) are higher than that for the pseudo-first-order model (R^2>0. 95), indicating that the present system can be well defined by the pseudo-second-order kinetic model in the adsorption step. Additionally, the theoretical equilibrium sorption capacity (qe,cal) calculated by the pseudo-second-order model at all concentrations are also in good agreement with those obtained from experiments (qe,exp). The fitness of the pseudo-second-order kinetic model reveals that the rate-limiting step in adsorption is controlled by chemical process (Lin *et al.,* 2016).

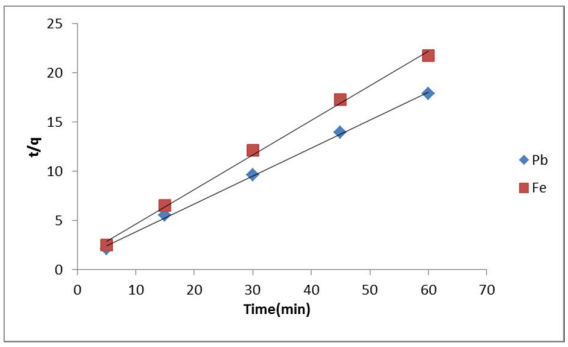

Fig. 8: Pseudo second order model for the exchange of Fe (II) and Pb(II) ions on MgAl-EDTA-LDH

Table. 2: Pseudo - First and second order parameters for the adsorption of Fe (II) and Pb(II) on MgAl-EDTA-LDH.

Metal Ions	$q_{e,cal.}$ (mg/g)	$q_{e,exp.}$ (mg/g)	$K_1\times10^{-2}$ (min^{-1})	R^2	$q_{e,cal}$ (mg/g)	$q_{e,exp.}$ (mg/g)	$K_2\times10^{-2}$ (gmg^{-1} min^{-1})	R^2
Fe^{2+}	68.24	32.11	0.192	0.953	28.49	32.11	19.219	0.994
Pb^{2+}	82.36	38.37	0.377	0.965	35.63	38.3	37.757	0.995

3.6. Adsorption isotherms

In order to gain better understanding of Fe (II) and Pb(II) adsorption mechanism and to quantify the adsorption data, two most widely used isotherms, Langmuir and Freundlich model, were employed to simulate the experimental data. The Langmuir isotherm model has been successfully used to various processes of monolayer adsorption (Langmuir, 1916). The model assumes that all activated sites on the adsorbent surface have equal affinity for adsorbate molecules. Once an adsorbate molecule occupies adsorption site, no further adsorption can occur there. The Langmuir model isexpressed in the following linear equation:

$$\frac{\mathrm{Ce}}{\mathrm{qe}} = \frac{1}{\mathrm{qmKL}} + \frac{1}{\mathrm{qmax}}\,Ce$$

Where qe (mg·g-1) is the amount of Fe (II) and Pb(II) adsorbed on the adsorbent at equilibrium, qmax (mg·g-1) denotes the maximum adsorption capacity corresponding to complete monolayer coverage, Ce ($mg\cdot L^{-1}$) is the equilibrium Fe (II) and Pb(II) concentration, and KL (L·mg-1) is the Langmuir adsorption constant.

The Freundlich isotherm model is an empirical equation assuming a heterogeneous surface and a multi-layer adsorption with an energetic nonuniform distribution (Jing *et al.,* 2019), and it can be expressed as follows:

$$\log q_e = \log k_f + (1/n) \log C$$

Where KF ((mg·g-1) Freundlich coefficient characteristic of the adsorption affinity of the adsorbent, and *n* is the linearity index.

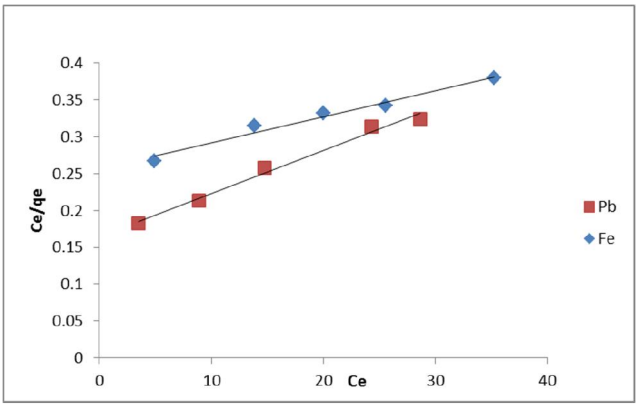

Fig. 9: plot of (Ce/qe) against Ce for Fe (II) and Pb(II) metals ions.

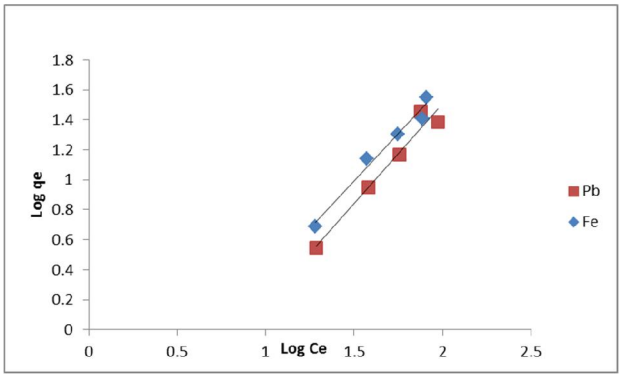

Fig. 10: plot of log q_e versus log C_e for Fe (II) and Pb(II) metals ions.

The fitting plots of Langmuir and Freundlich isotherm models for Fe (II) and Pb(II) adsorption onto MgAl-EDTA-LDH are depicted in Figs. 9,10 and the calculated isotherm parameters are listed in Table 3. It is observed that the correlation coefficients of Langmuir isotherm model are higher than that of Freundlich isotherm model, indicating that the adsorption data follows the Langmuir isotherm and the adsorption is a monolayer adsorption process. The maximum theoretical adsorption capacities of Fe (II) and Pb(II) calculated from the Langmuir model are 85.71, and 109.21 mg g-1, respectively, .In addition, the Langmuir constant KL has positive value and the Freundlich constant n (1.254-1.233) lies in the range of 1-10, suggesting a favorable adsorption system (Yang *et al.,* 2019). One of the essential characteristics of Langmuir equation can be expressed by a dimensionless constant, RL, which is also called equilibrium parameter or separation factor and can be defined as:

$$R_L=\frac{1}{1+CoKL}$$

The RL value indicates the type of isotherm to be unfavorable (RL>1), linear (RL=1), favorable (0<RL<1) and irreversible (RL=0) (Li *et al.,* 2009). It can be observed from Table 3 that the RL values are in the range of 0 to 1, indicating a favorable adsorption of Fe (II) and Pb(II) on MgAl-EDTA-LDH.

Table 3: Regression parameters for the Langmuir and Freundlich isotherms for solutions of Fe (II) and Pb(II)

Metals	Langmuir constants (MgAl-EDTA-LDH)				Freundlich constants (MgAl-EDTA-LDH)		
	Q_{max} (mg/g)	K_L	RL	R^2	K_F	n	R^2
Fe^{2+}	85.71	0.0136	0.269	0.983	7.654	1.25	0.976
Pb^{2+}	109.21	0.0169	0.228	0.987	14.125	1.23	0.962

Table 4: Comparison of the maximum adsorption capacity of heavy metals onto different adsorbents

Adsorbent	q_m (mg/g)	Ref.
ZnAl-EDTA for Cu^{2+}	223	6
AminoTrimethylene Phosphonic Acid-LDH for Cu^{2+}	42.02	7
AminoTrimethylene Phosphonic Acid-LDH for Pb^{2+}	84.06	7
EDTA-LDH/PVA for Cd^{2+}	81.76	10
LDH-EDTA for Cr(VI)	47.62	11
LDH-EDTA-acrylamide for Cr(VI)	48.47	18
diethyldithiocarbamate -LDH for Cr(VI)	52	21
MgAl-EDTA-LDH for Fe^{2+}	85.71	This study
MgAl-EDTA-LDH for Pb^{2+}	109.21	This study

3.7. Application

Abu Rawash, is located within the Northwest part of Cairo. The Quaternary aquifer occupies the northern and northeastern parts and represents the main water-bearing unit in the area locating east of Abu Rawash. The Quaternary aquifer water contains heavy metals. From the chemical analysis of the five waste water samples it is clear that, the soluble heavy metals of waste water samples such as Lead and iron are more than the permissible limit (0.05 mg/l and 0.3 mg/respectively) To overcome this problem, two of waste water samples were chosen for the treatment process. The efficiency of the treatment was measured by chemical analysis samples before and after this process using MgAl-EDTA-LDH. It was found that the soluble Lead in samples was 0.583 ppm before treatment and 0.004 ppm after treatment, and 0.697 ppm before treatment and 0.009 ppm after treatment and the soluble iron in samples was 1.321 ppm before treatment and 0.187 ppm after treatment, and 0.826 ppm before treatment and 0.082 ppm after treatment .It can be concluded that the surfaces of MgAl-EDTA-LDH had adsorption sites that were able to bind Lead and iron ions.

4. Conclusions

MgAl-EDTA-LDH was successfully synthesized and used as adsorbent for Fe (II) and Pb (II) removal from aqueous solutions. The physicochemical properties of the adsorbents were determined by using SEM, XRD and FTIR. Some important parameters that influence Fe (II) and Pb(II) adsorption from aqueous solutions using MgAl-EDTA-LDH. The results show that the MgAl-EDTA-LDH composite exhibited a high adsorption capacity and efficient adsorption toward Fe (II) and Pb(II) in aqueous mediums within a wide solution pH range. The pseudo-second-order model was the most suitable kinetic model. The isotherm analysis suggested that the adsorption data could be represented by the Langmuir model and the maximum adsorption capacity calculated were 85.71 $mg \cdot g^{-1}$ And 109.21 $mg \cdot g^{-1}$ for Fe (II) and Pb(II) respectively. It can be concluded that the surfaces of MgAl-EDTA-LDH had adsorption sites that were able to bind Lead and iron ions.

Funding

"This research received no external funding"

References

Ahmed, M.D., 2018. Remove heavy metals from groundwater using carbon nanotubes grafted with amino compound, Journal of Separation Science and Technology, 4016-4022. DOI:10.1080/01496395.2018.1441304.

Arshid, B., A.M. Lateef, A. Sozia, M. Taniya, A.B. Mudasir, G.N. Dar and H.P. Altaf, 2019. Removal of heavy metal ions from aqueous system by ion‑exchange and biosorption methods, Environmental Chemistry Letters, 17:729–754. https://doi.org/10.1007/s10311-018-00828-y

Asma, Rafiq, I.S.A. Muhammad, N. Faiza, K. Maaz, K. Qasim, and M. Muhammad, 2021. Photocatalytic degradation of dyes using semiconductor photocatalysts to clean industrial water pollution, Journal of Industrial and Engineering Chemistry, 97:111-128. https://doi.org/10.1016/j.jiec.2021.02.017.

Bansod, B.K., T. Kumar, R. Thakur, and S. Rana, 2017. A review on various electrochemical techniques for heavy metal ions detection with different sensing platforms. Biosens. Bioelectron. 94: 443–455. https://doi.org/10.1016/j.bios.2017.03.031

Bolan, S., A. Kunhikrishnan, B. Seshadri, G. Choppala, R. Naidu, N.S. Bolan, Y.S. Ok, M. Zhang, C.-G. Li, and F. Li, 2017. Sources, distribution, bioavailability, toxicity, and risk assessment of heavy metal (loid)s in complementary medicines, Environ. Int. 108: 103-118. https:// doi.org/10.1016 /j.envint.2017.08.005

Camilo, Z.-L., N.-B. Daniela, F. Freddy, Z.-L. Ezequiel, N. Ming, A. Frank, and H.G. Victor, 2021. metal water pollution: A fresh look about hazards, novel and conventional remediation methods. J. Environmental Technology & Innovation, Volume 22, 2021, 101504 https ://doi. org/10.1016 /j.eti.2021.101504

Dhal, B., H.N. Thatoi, N.N. and B.D. Das, 2013. Pandey Chemical and microbial remediation of hexavalent chromium from contaminated soil and mining/metallurgical solid waste: A review. Journal of Hazardous Materials, 250–251: 272–291. https://doi.org/10.1016/j.jhazmat.2013.01.048

Eslam, R.S. , Yousra H.K. , R.S. Eglal, A.G. Khairia, and G.M.B. Reda, 2019. Development the sorption behavior of nanocomposite Mg/Al LDH by chelating with different monomers , Composites Part B, 175: 107131. https://doi.org/10.1016/j.compositesb.2019.107131

Facui, Y., S. Shiqi, C. Xiaoqi, C. Yue, Z. Fei, and L. Ziqiang, 2016. Mg–Al layered double hydroxides modified clay adsorbents for efficient removal of Pb^{2+}, Cu^{2+} and Ni^{2+} from water, Applied Clay Science , 123: 134–140. doi.10.1016/j.clay.2016.01.026

Hai, N.T., L. Chu-Ching, H.W. Seung, and C. Huang-Ping, 2018. Efficient removal of copper and lead by Mg/Al layered double hydroxides intercalated with organic acid anions: Adsorption kinetics, isotherms, and thermodynamics. Applied Clay Science, 154: 17–27. https://doi.org/10.1016/j.clay.2017).12.033.

Hong, C., L. Jianhui, Z. Ning, C. Liangzhe, Z. Shuiping, W. Yao, Z. Wengong, and L. Qidan, 2018. Preparation of MgAl-EDTA-LDH based electrospun nanofiber membrane and its adsorption properties of copper(II) from wastewater, Journal of Hazardous Materials 345,1–9. DOI:10.1016/j.jhazmat.2017.11.002

Jing, L., Y. Haiqin, Z. Xue, Z. Rixin, and Y. Liangguo, 2020. Crosslinking acrylamide with EDTA-intercalated layered double hydroxide for enhanced recovery of Cr (VI) and Congo red: Adsorptive and mechanistic study, Environ. Sci. Eng. 14(3): 52. DOI:10.1007/s11783-020-1229-x

Jing, L., Y. Liangguo, Y. Yanting, Z. Xue, Z. Rixin and Y. Haiqin, 2019. Insight into the adsorption mechanisms of aqueous hexavalent chromium by EDTA intercalated layered double hydroxides: XRD, FTIR,XPS, and zeta potential studies, New J. Chem., 43:15915, DOI: 10.1039/c9nj03479j.

Jing, M., Q. Guotong, and Y. Zhang, 2018. Heavy metal removal from aqueous solutions by 664 calcium silicate powder from waste coal fly-ash. J. Clean. Prod., 182:776-782. https://doi.org/10.1016/j.jclepro.2018.02.115

Jingwan, H., M. Xiaopeng, and W. Yin, 2021. Zirconium-modified natural clays for phosphate removal: Effect of clay minerals, j.Environmental Research, 110685. https:// doi.org/10.1016/j. envres .2020.110685.

Langmuir, I., 1916.The constitution and fundamental properties of solids and liqiuds. Part I. Solids, J. Am. Chem. Soc. 38:2221-2295. https://doi.org/10.1021/ja02268a002

Li, Y., B. Gao, T. Wu, D. Sun, X. Li, B. Wang, and F. Lu, 2009. Hexavalent chromium removal from aqueous solution by adsorption on aluminum magnesium mixed hydroxide, Water Res. 43: 3067-3075. https://doi.org/10.1016/j.watres.2009.04.008.

Lin, D., S. Zhou, W. Li and Z. Shiqing, 2016. Fabrication of a novel $NiFe_2O_4$/Zn-Al layered double hydroxide intercalated with EDTA composite and its adsorption behavior for Cr(VI) from aqueous solution, Journal of Physical and Chemistry of Solids, S0022-3697(16)30679-5 http://dx.doi.org/10.1016/j.jpcs.2016.12.030.

Lu, X., L. Jianyue, and G. Jinwen, 2021. Dynamic game in agriculture and industry cross-sectoral water pollution governance in developing countries. J. Agricultural Water Management, 243, 106417. https://doi.org/10.1016/j.agwat.2020.106417

Mohammad, D., H. Atefeh, and A. Parvin, 2019. Facile synthesis of ZnAl-EDTA layered double hydroxide/poly(vinyl alcohol) nanocomposites as an efficient adsorbent of Cd(II) ions from the aqueous solution, Applied Clay Science 170: 21–28. https://doi.org/10.1016/j.clay.2019.01.007

Naja, G.M., and B. Volesky, 2009. Toxicity and sources of Pb, Cd, Hg, Cr, As, and radionuclides in the environment, Heavy Met. Environ. 8, DOI:10.1201/9781420073195.ch2

Naoki, K. and Z. Shuang, 2018. Adsorption of Heavy Metals on Layered Double Hydroxides (LDHs) Intercalated with Chelating Agents, Advanced Sorption Process Applications, Serpil Edebali, Intech Open, DOI: 10.5772/intechopen.80865.

Pavlovic, I., C. Barriga, M.C. Hermosín, J. Cornejo, and M.C. Ulibarri, 2005. Adsorption of acidic pesticides 2,4-D, Clopyralid and Picloram on calcined hydrotalcite. Appl. Clay Sci. 30: 125–133. DOI:10.1016/j.clay.2005.04.004

Pourret, O., and J.C. Bollinger, 2018. What to do now: to use or not to use? Sci. Total Environ. 610 (611):419–420. DOI:10.1016/j.scitotenv.2017.08.043.

Rajib, L.G. , S. Pinaki, G.B. Krishna, and K.D. Dipak, 1998. Adsorption of Cr (VI) in layered double hydroxides, Applied Clay Science, 13: 21–34 https://doi.org/10.1016/S0169-1317(98)00010-6

Reza, R.F., S. Pajoum, T. Omid and E. Fariborz, 2021. Fabrication of a new reactor design to apply freshwater mussel Anodonta cygnea for biological removal of water pollution, J. Aquaculture, 544: 737077, https://doi.org/10.1016/j.aquaculture.2021.737077

Sidi, Z., A.K. Muhammad, W. Fengyun, B. Zahira, and X. Mingzhu, 2020. Rapid Removal of Toxic Metals Cu^{2+} and Pb^{2+} by Amino Trimethylene Phosphonic Acid Intercalated Layered Double Hydroxide: A Combined Experimental and DFT Study, Chemical Engineering Journal, 392: 12371. doi.org/10.1016/j.cej.2019.123711.

Wen, J., Y. Fang, and G. Zeng, 2018. Progress and prospect of adsorptive removal of heavy metal ions from aqueous solution using metal–organic frameworks: a review of studies from the last decade, Chemosphere, 201:627-643. https://doi.org/10.1016/j.chemosphere.2018.03.047

Yang, J., L. Cang, Q. Sun, G. Dong, S.T. Ata-Ul-Karim, and D. Zhou, 2019.Effects of soil environmental factors and UV aging on Cu^{2+} adsorption on microplastics, Environ. Sci. Pollut. Res. () 1-10. DOI:10.1007/s11356-019-05643-8

Yang, J., Z. Yingshuang, F. Jiangang Y., Liangxiao, L. Zheng, L. Chang, Z. Di, and W. Xiaobo, 2019. A novel magnetic biochar/MgFe-layered double hydroxides composite removing Pb^{2+} from aqueous solution: Isotherms, kinetics and thermodynamics, Colloids and Surfaces A 567: 278–287, https://doi.org/10.1016/j.colsurfa.2019.01.064.

Yuan, X.Y., Y.F. Wang, J. Wang, C. Zhou, Q. Tang, and X.B. Rao, 2013. Calcined graphene/MgAl-layered double hydroxides for enhanced Cr (VI) removal. Chemical Engineering Journal, 221: 204–213. https://doi.org/10.1016/j.cej.2013.01.090

Zaghloul, A., R. Benhiti, A. Soudani, M. Chiban, M. Zerbet, and F. Sinan, 2019. Removal of methyl orange from aqueous solution using synthetic clay type MgAl-LDH: Characterization, Isotherm and thermodynamic studies. Mediterranean Journal of Chemistry, 9:155-163. http://dx.doi.org/10.13171/mjc92190925728fs.

Zhou, L., M. Slaný, B. Bai, W. Du, C. Qu, J. Zhang, and Y. Tang, 2021. Enhanced Removal of Sulfonated Lignite from Oil Wastewater with Multidimensional MgAl-LDH Nanoparticles. Nanomaterials, 11: 861. https://doi.org/10.3390/nano 11040861 A